



Structural Behavior Of thin ferrocement plates with and without stiffeners subjected to compression loading

Yousry I.B. Shahren¹, Zeinab A. Etman¹, Osama Gomaa²

¹Department of Civil Engineering - Faculty of Engineering- Menoufia University, Egypt

²Msc. Fellow, civil Engineer

يهدف هذا البحث الى دراسة السلوك الانشائي للألواح الفيروسيمنية الرقيقة السمك تحت تأثير أحمال الضغط بدون تقوية ومع وجود تقوية لهذه الألواح. ويتناول بحثنا كيفية انتاج الألواح الفيروسيمنية الرقيقة وتركيبها باعتبارها عناصر معرضة لأحمال ضغط يتم صبها اولاً في المعمل. ويشتمل البحث علي برنامج عملي قائم علي صب عدد (12) من الألواح الرقيقة الفيروسيمنية بمساحة 1 متر مربع وبسمك 25 مم. وقد تم صب بعض الألواح باستخدام صلب التسليح فقط واخري باستخدام الشبك المعدني الممدد والملحوم فقط و باقي الألواح باستخدام الشبك المعدني الممدد مع صلب التسليح. وكانت المتغيرات محل الدراسة تشمل استخدام تقوية ومع عدم وجود تقوية للألواح بالاضافه الى نوع التسليح وعدد طبقات التسليح و أجريت التجارب المعملية على الألواح تحت تأثير حمل الضغط وتشغيل اقصى حمل من خلال تطبيق حمل هيدروليكي حتي حدوث الانهيار ، وقد تم قياس الترخيم عند منتصف اطراف الألواح ، وحساب واستنتاج أحمال التشرخ ، وأقصى حمل وقياس المساحة تحت منحنى الحمل والترخيم لقياس الطاقة المخزنة. وقد تم استخدام أحد برامج التحليل الانشائي (ANSYS 15) ومقارنة النتائج العملية بالنظرية.

ABSTRACT

Ferrocement plates with or without stiffeners are presented for use as a retaining wall or flood protection. These plates are lighter than the reinforced concrete plates. The present study focused on the structural behavior of thin ferrocement plates with and without frame subjected to axial compression loading. For this objective, an experimental program was carried out and a finite element model with ANSYS15 was adopted. A total of twelve samples thin ferrocement plates 50 mm in thickness, 1000 mm in width and 1000 mm in length were tested under compression loading up to failure. The main variables taken into consideration in this paper were the type of reinforcement (reinforced bar and welded steel wire meshes), a number of layers of steel meshes (one layer, two layers, three layers and four layers) and the direction of load. The behavior of the tested thin plates was investigated with special attention to initial cracking, ultimate load, the deflection under different stages of loading, cracking pattern, energy absorption and ductility index. Good agreement was found compared with the experimental results. The results illustrated that good performance of the ferrocement plates and this may be of true construction advantages

Keywords: ferrocement, welded wire mesh, thin plates, compression loading, ductility index, energy absorption, ANSYS 15.

1 INTRODUCTION

Ferrocement construction technology is quite popular throughout the world. In the 1999, the American Concrete Institute ACI committee 549 [1] published a general definition of ferrocement states that "Ferrocement is a type of thin wall reinforced concrete commonly constructed of hydraulic cement mortar reinforced with closely spaced layers of continuous and relatively small size wire mesh. The mesh may be made of metallic or other suitable materials". A literature review was presented by Sakthivel P.B. and Jagannathan A. [2] and Apostolos Koukouselis, Euripidis Mistakidis [3] on ferrocement as a construction materials. Madhuri N. Savale and P. M. Alandkar [4]

studied the behaviour of ferrocement plates due to shear force. Finite element analyses using (ANSYS) was conducted. They resulted that as increasing the volume fraction (VF) of the wire mesh layer subsequently increases the shear carrying capacity of the plate. Many researchers studied the behavior of ferrocement elements under different applied load up to failure [5-7]. Nassif and Najm [8] investigated an experimental and a theoretical model for ferrocement-concrete composite beams. Various types of reinforced concrete beam overlaid on a thin section of ferrocement (cement paste and wire mesh) were tested up to failure under two-point loading system. Their results showed that the proposed composite beam has good ductility, cracking strength and ultimate capacity more than reinforced concrete beam. S. Bhalsing et. al. [9] studied the tensile strength behavior of ferrocement due to the specific surface area. A relation between the tensile strength of ferrocement and its mechanical properties were determined. Desai, 2011 [10] reported that cement matrix of ferrocement does not crack. This is due to cracking forces are taken over by wire mesh reinforcement immediately below the surface. Using ferrocement in some applications as swimming pools and water tanks, silos, corrugated roofs, shell and dome structures, and also in the repair of old/ deteriorated RCC structures was illustrated. Ferrocement can be fabricated into any desired shape or structural configuration that is generally not possible with standard masonry, RCC or steel [11]. Ferrocement is being explored as building materials substituting stone, brick, RCC, steel, prestressed concrete and timber and also as structural components walls, floors, roofs, beams, columns and plates, water and soil retaining wall structures; other applications include window and door frames and shutters [12]. Ferrocement was used for construction many structures such as housing units, shell roofs, water tanks and swimming pools, biogas digesters, silos, food storage units. Also, some specialized applications such as floating marine structures for which reinforced concrete is too heavy, ferrocement is a preferred choice over reinforced concrete. Considering all these points in view, the present study focused on the behavior of plates with frame and without frame. For this purpose two series of plates executed subjected to uniform axial compression load carried out to study. First crack, serviceability, ultimate loads, ductility ratios and energy absorption properties of all the tested plates up to final failure have been studied. Out of this research, it can be applied in the construction of retaining walls and flood protection.

2 Research significant

This paper introduces a new effective of thin ferrocement plates with and without frame subjected to uniform axial compression loading. Welded steel wire meshes as reinforcement are used as an alternative to ordinary reinforcement. The objectives of the experimental program described within this research were (i) Behavior of thin ferrocement plates with and without frame subjected to uniform axial compression loading. (ii) Studying the effect of the type of reinforcement, a number of layers of welded steel wire meshes (one layer, two layers, three layers and four layers) on the structural behavior of thin ferrocement plates (iii) Direction of loading. Theoretical analysis will be conducted by ANSYS 15 as a finite element package to verify the results of the experimental program.

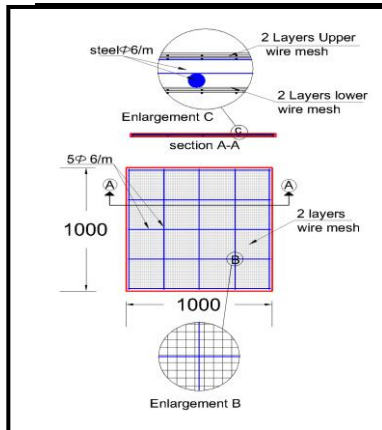
3 Experimental Program

To evaluate the aim of this study, an experimental program, including the test of twelve thin ferrocement plates was conducted. Fixed supported thin ferrocement plates dimension 1000 mm × 1000 mm with 50 mm thickness. The geometrical and reinforcement details

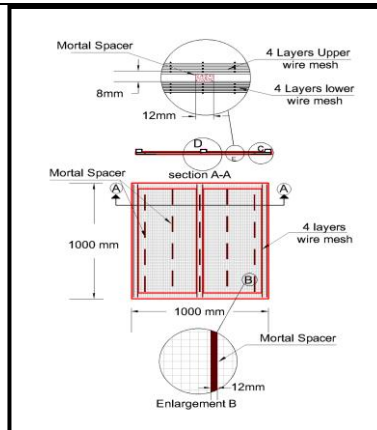
of the tested plates are shown in Table 5 as well as Figure 15 and Figure 16. The following code was used for the sample designation. the letter C refers to the control specimen, the letter F refers to the specimen have frame, the letter S define the steel reinforcement moreover the following number refer to the number of steel bars in each direction, the letter W is for welded steel wire mesh furthermore the following number refer to the lower and upper number of layers wire mesh. Letter L refers to the direction of loading.

Table 5 :Details of the tested specimens

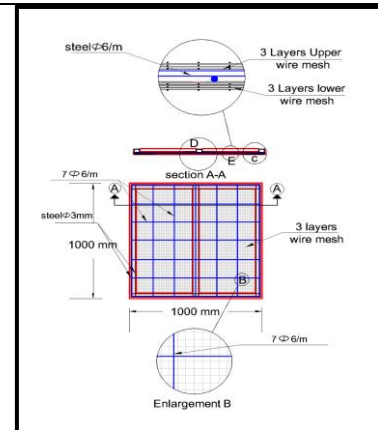
CODE	steel wire mesh		Reinforcement steel bars			Plate weight, (ton)
	No. of layers	Vf	steel bars	No. of steel bars		
S5W2	2	0.00438	Φ6/m	5	without frame	0.5969
FW4	4	0.01517	-	-		0.7447
FS7W3	3	0.01138	Φ6/m	7	with frame	0.7345
FCS7	-	-		7		0.6534
FW3	3	0.01138	-	-		0.6925
FS5W2	2	0.00759	Φ6/m	5		0.4849
W4	4	0.00657	-	-		0.5646
CS7	-	-		7		0.4939
S7W3	3	0.00657	Φ6/m	7	without frame	0.5932
S7W2	2	0.00438		7		0.478
W3	3	0.00876	-	-		0.6181
FS7W3L	3	0.01138	Φ6/m	7	with frame	0.7345



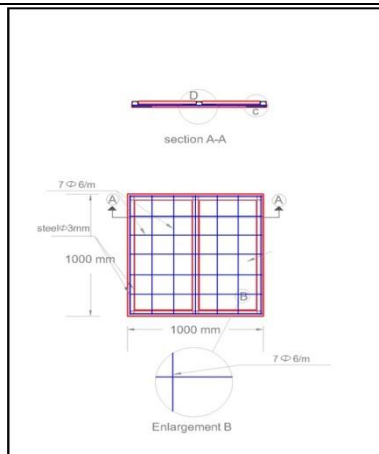
Reinforcement details of S5W2



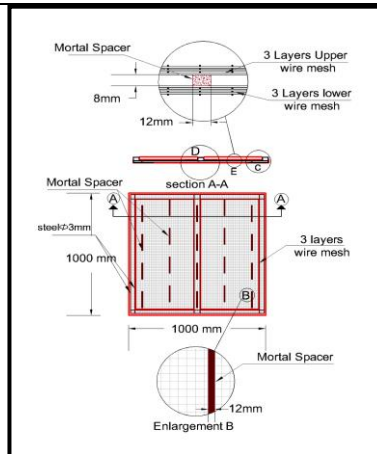
Reinforcement details of FW4



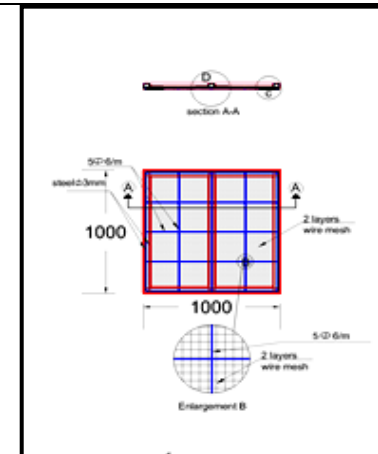
Reinforcement details of FS7W3.



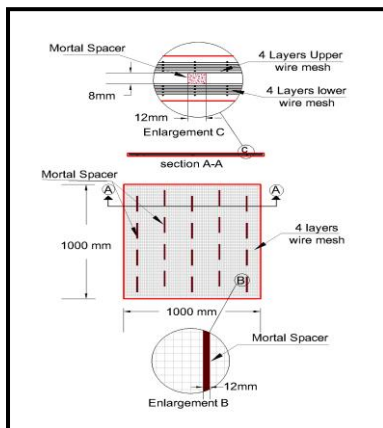
Reinforcement details of FCS7



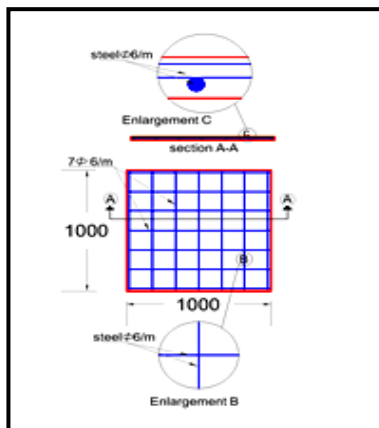
Reinforcement details of FW3



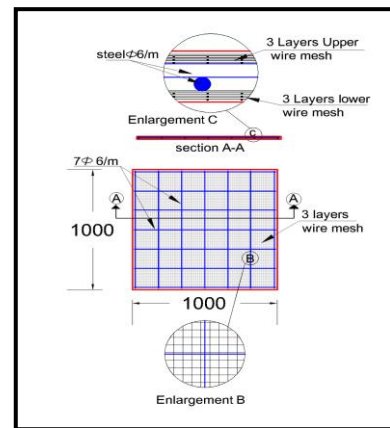
Reinforcement details of FS5W2



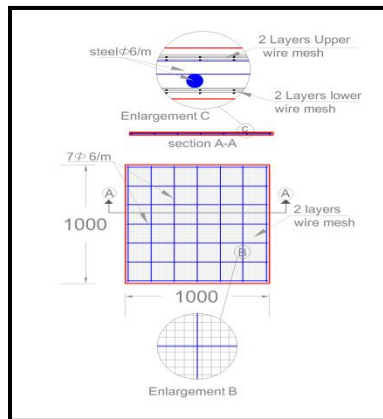
Reinforcement details of W4



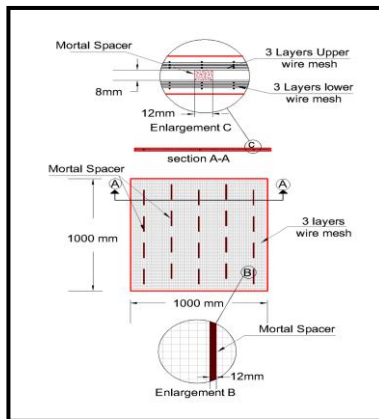
Reinforcement details of CS7



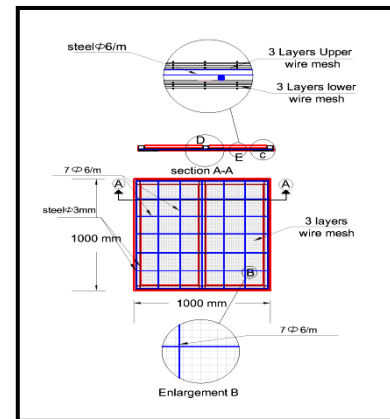
Reinforcement details of S7W3



Reinforcement details of S7W2

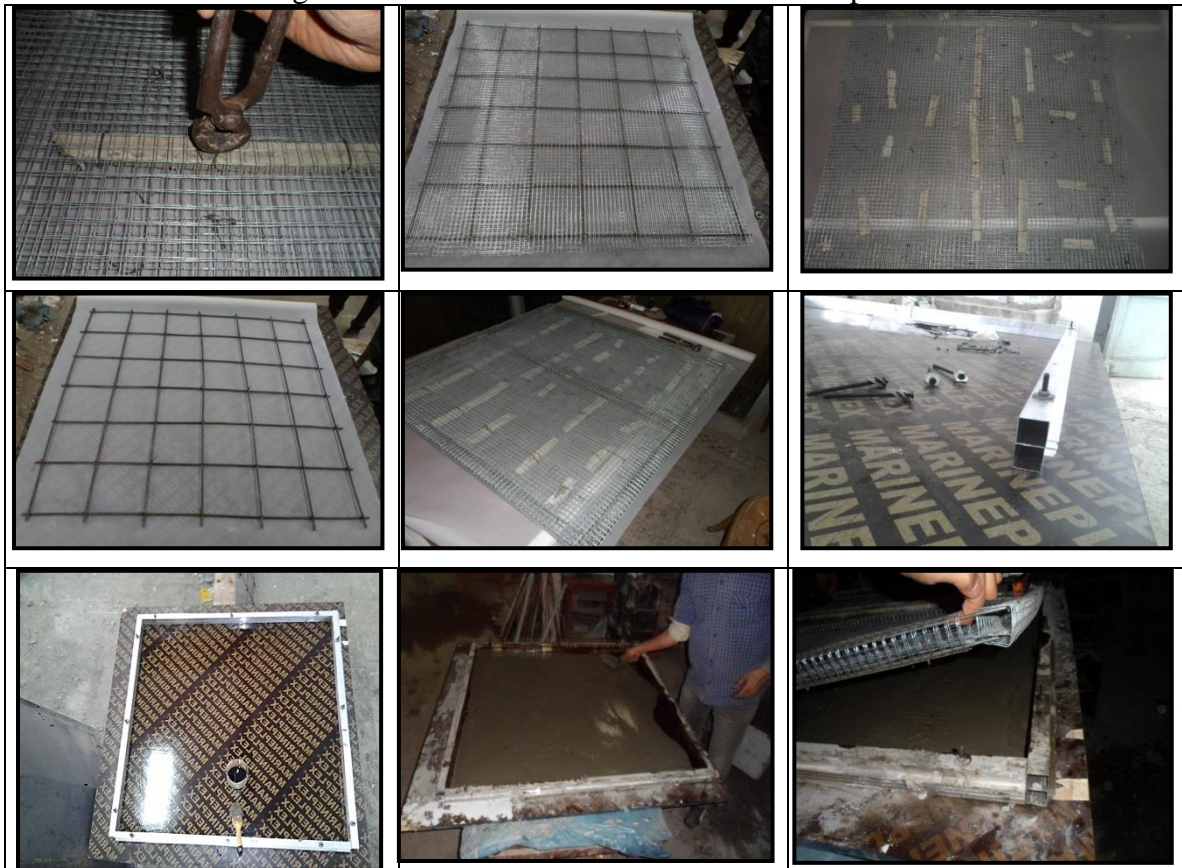


Reinforcement details of W3.



Reinforcement details of FS7W3L

Figure 15: reinforcement details of the tested plates



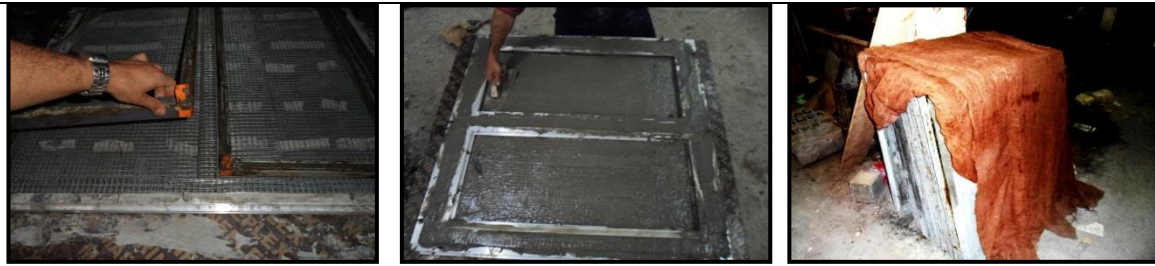


Figure 16: Procedures of cast ferrocement plates

3.1 Material Properties

Ordinary Portland cement type (CEMI 42.5N) according to the requirements of E.S.S.4756-11, 2009 [13] with a specific gravity of 3.15 and a specific surface area (Blaine fineness) 3700cm²/gm. was used. Locally produced identified Silica Fume(S.F.) was delivered in 25-Kg sacks according to the manufacturer; the powder had an average particle size of 0.1 micrometer, specific surface area 170000 cm²/gm. and specific gravity of 2.2. Natural siliceous sand was used as fine aggregate throughout the current research. The fine aggregates used was obtained from Suez zone with 2.59 specific gravity and 2.63 fineness modulus of and the percentage of particles finer than sieve No. 200 resulted absorption percentage of 0.79%. High range water reducer (HRWR) of a synthetic type dispersion base was used to improve the mixes workability. HRWR complies with ASTM C494 Type A&F [14]. The polypropylene fibers were fibrillated as shown in Figure 17 complies with ASTM C1116 [15]. The properties of polypropylene fibers according to the manufacture data sheet was illustrated in **Table 6** . Welded steel wire mesh as shown in Figure 18 was used. **Table 7** shows the geometric and mechanical properties of the welded steel wire meshes. The mechanical properties of the welded wire mesh comply with of ACI 549.1R-97 [1]. Mild steel rebar (nominal diameters 6 mm) was used as reinforcement. The rebar had yield and ultimate tensile strength of 250 and 385 MPa, respectively.



Figure 17: polypropylene fiber

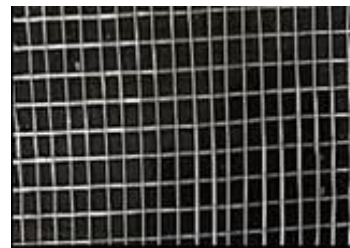


Figure 18: Welded Wire Mesh

Table 6: properties of the polypropylene fibers according to the manufacture data sheet.

Length, mm	Specific gravity, gm/cm ³	Diameter, micron	Modules of elasticity, Gpa	Tensile strength, N/mm ²	Tensile elengation
15	0.91	25	1.6	395	25

Table 7 : geometric properties of the welded steel wire meshes.

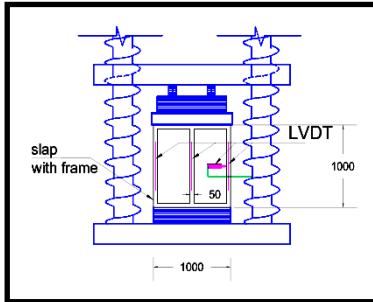
Dimensions, mm		Diameter, mm	Weight, gm/m ²	Proof stress, N/mm ²	Ultimate strength, N/mm ²	Ultimate strain × 10 ⁻³	Proof strain × 10 ⁻³
Long way	Short way						
12.5	12.5	0.695	430	737	834	58.8	1.17

Table 8 : Mix proportions (Kg/m³)

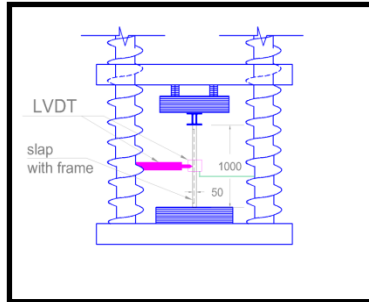
Cement	Sand	HRWR	S.F.	Water	Fiber	F _{cu} (MPa), 28 days
670	1340	3.35	67	234.5	6.7	30
S.F.= silica fume				HRWR = High range water reducer		

3.2 Experimental test set-up

A hydraulic jack was used to apply the uniform vertical load at the center of each plate as shown from Figure 19 to Figure 25. The load was transferred uniformly to Plates using Steel beam. The purpose of the steel beam was to evenly distribute the concentrated Load at the end section and to prevent premature local failure. A load cell was used to measure the applied load. A total of five LVDTs were installed to measure the deformation of each Specimen. Four LVDTs were located perpendicular to plate, while additional LVDT was positioned in plan at each plate.



(a) Elevation view

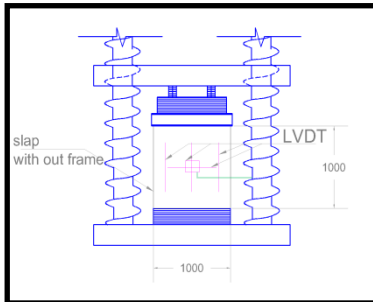


(b) Side View

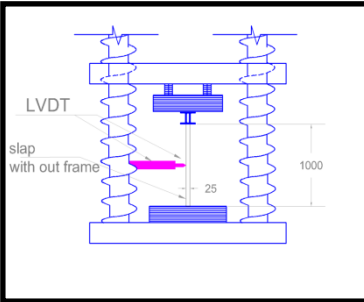
Figure 19: Test setup and the position of the LVDTs with frame plate



Figure 20: Four LVDTs for measuring displacement in the plan view 1.



(a) Elevation view



(b) Side View

Figure 21: Test setup and the position of the LVDTs without frame plate



Figure 22: Test setup and the position of the LVDTs with frame plate elevation view.



Figure 23: Test setup and A hydraulic jack



Figure 24: Data logger accuracy to .001 mm



Figure 25: Lateral deflections (LVDTs)

4 Experimental Results and Discussions

The obtained results for the initial cracking load, ultimate load, maximum deflection at ultimate load index and energy absorption as shown in Table 9. Ultimate load and deflection at ultimate load were measured and obtained during the test, while ductility index and energy absorption were determined from the load-deflection diagram for each tested plates.

Table 9: First crack, ultimate loads, ductility ratios and energy absorption properties of all the tested plates.

Plate No.	Code	Initial cracking load, kN	Ultimate load, kN	Ductility, mm		Ductility index	Energy absorption, KN.mm	service ability load
				$\Delta_{ult.}$	$\Delta_{init.}$			
S1	S5W2	32	105.50	7	2.91	2.41	441	65
S2	FW4	114	406.84	4.1	0.69	5.94	1626	254
S3	FS7W3	120	398.93	6.0	1.53	3.93	1400	249
S4	FCS7	146	363.98	1.2	0.53	2.23	194	227
S5	FW3	121	346.84	3.4	1.76	1.93	1257	216
S6	FS5W2	77	193	8.8	3.45	2.548	777	121
S7	W4	74	230.13	12.0	1.40	8.57	1248	143
S8	CS7	90	95.216	4.0	1.19	3.38	162	59
S9	S7W3	54	150.34	11.0	0.69	15.88	275	93
S10	S7W2	36	116.7	8.0	1.17	6.86	224	73
S11	W3	53	146.39	10.4	1.93	5.39	847	91
S12	FS7W3L	77	208.36	2.0	0.06	35.35	129	130

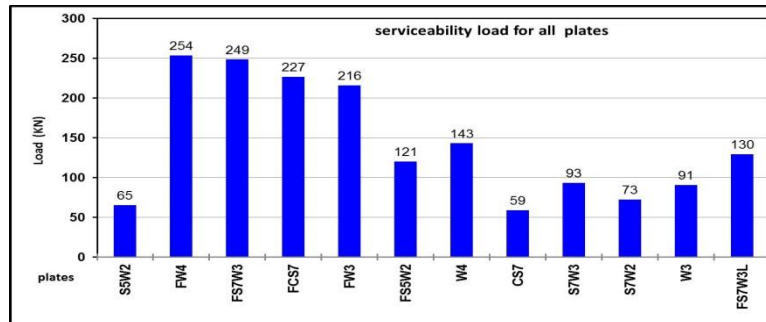


Figure 26: serviceability load for all plates

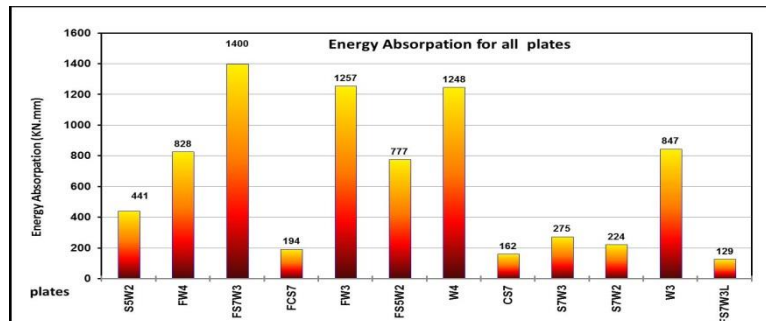


Figure 27: Energy absorption, KN.mm for all plates

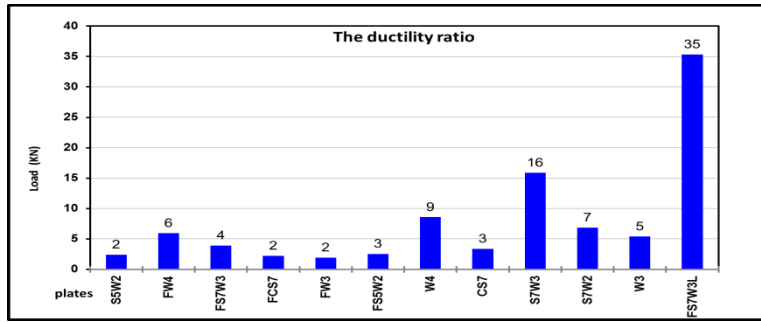


Figure 28: Ductility index for all plates

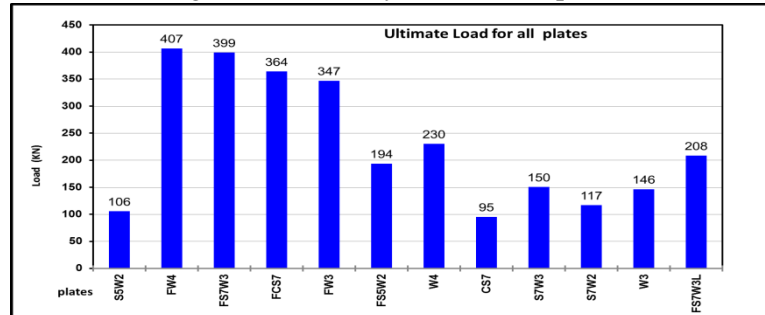


Figure 29: Ultimate load for all plates

4.1 Effect of type of reinforcement

Figure 30 and Figure 31 show the effect of types of reinforcement on the behavior of the tested plates with and without frame. From these figures, the loads for conventional reinforcement were the lowest compared with the plates reinforced with the steel wire meshes only or reinforced with steelwires and conventional reinforcement. However the energy absorption for the plates reinforces with steel wire meshes is higher than that reinforced with convention reinforcement. The deflection of the plates was decreasing by increasing area of the reinforcement of these plates. Moreover, as the Volume of reinforcement were little big as the stiffness of the plates were higher, and consequently the deflections were small. Increasing the volume of reinforcement not necessarily increasing the ultimate load the cracking load, but consequently delayed the sudden reduction of stiffness of the plates depended on the surface area of reinforcement. The higher in addition to surface area of reinforcement was not necessarily have the higher of stiffness. as illustrated in Figure 30, the initial cracking load for (S9) and (S11) increased by 50% and 46%, respectively compared with (S8). Moreover the ultimate load increased by 58% and 54 %, respectively. The results were recorded for the plates with frame; a decreasing in the initial cracking by 18% and increasing ultimate load by 10 % for the plates (S3) which is reinforced with three layers wire mesh and traditional reinforcement compared with the plate (S4) which is reinforced with conventional reinforcement as as illustrated in Figure 31. In addition to the energy absorbed and ductility index were increased by 622% and 77%. For framed plates (S5) which is reinforced with steel wire mesh only compared with plates (S4); a decreasing in the initial cracking, ultimate load and ductility index by 26%, 5% and 13% were recorded but the energy absorbed increased by 289%

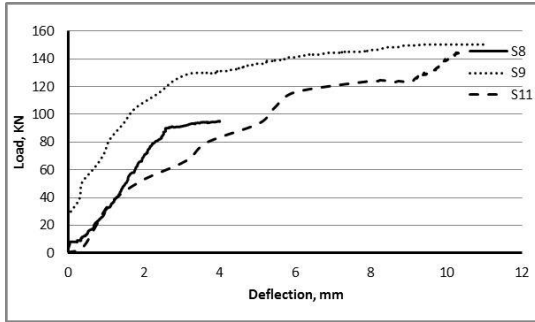


Figure 30: Effect of type of reinforcement on the load-deflection for the plates Without frame

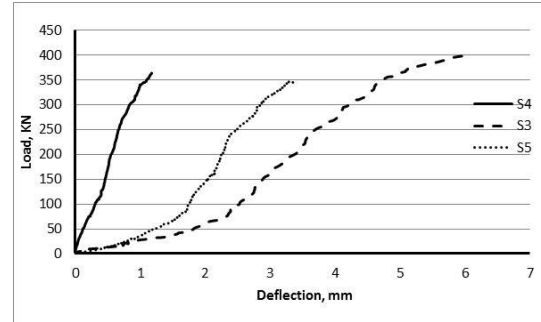


Figure 31: Effect of type of reinforcement on the load-deflection for the plates With frame

4.2 Effect of numbers of layers

The effect of numbers of steel wire mesh layer are shown in Figure 32 and Figure 33. As the numbers of steel wire mesh were increasing, the initial cracking, ultimate load, ductility index and energy absorptions increases. On the other hand, The deflection of the plates was inversely proportional to number of layers. Regards to plates without frame; the initial cracking load, ultimate load, ductility index and energy absorption increased by 40%, 57%, 59% and 47% for the four steel wire mesh layers (S7) compared with three wire mesh layers (S11), respectively as shown in Figure 32. Moreover plates with frame initial cracking load, ultimate load, ductility index and energy absorption increased by 6%, 17%, 208% and 29 % for the four mesh layers compared with three mesh layers respectively as illustrated in Figure 33.

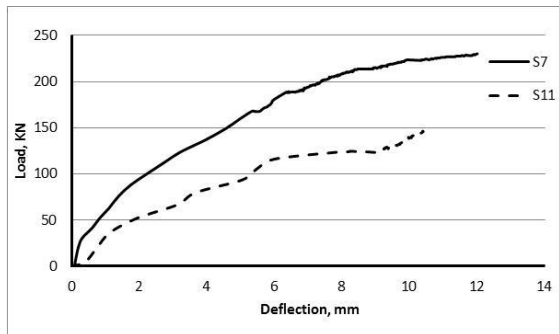


Figure 32: Effect of number of layer of wire mesh for the plates without frame

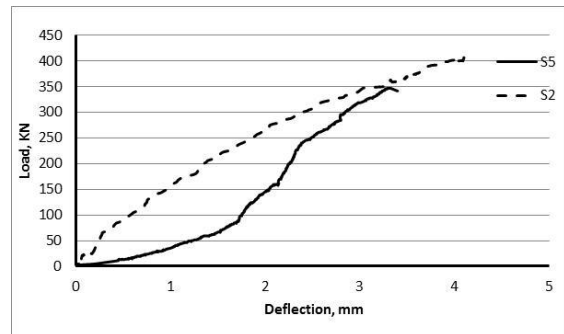


Figure 33: Effect of number of layer of wire mesh for the plates with frame

4.3 Effect of using of web

The effect of using web on the behaviour of plates is shown in Figure 34 to Figure 38. From those figures an improving were noticed for the behaviour for the paltes with frame compared with the plates without frame. Also, an improvement were found in the ductility index and energy absorbtion. Figure 34 illustrates the load-deflection curve for the plates (S1) and (S6). 145% , 84% , 6% and 76% increasing in initial cracking load, ultimate load, ductility index and energy absorbtion, respectively for plate (S2) with frame compared with plate (S7) without frame as shown in Figure 35. 55% and 77% increasing in initial cracking load, ultimate load but decrease in ductility index and energy absorbtion by 31% and 34% . For plate (S4) with frame compare with plate (S8) without frame 302%, 282% and 20% increasing in initial cracking load, ultimate load

and energy absorbtion but decrease in ductility index by 34% as shown in Figure 36. For plate (S3) with frame compare with plate (S9) without frame 121%, 165% and 410% increasing in initial cracking load, ultimate load and energy absorbtion but decrease in ductility index by 75% as shown in Figure 37. For plate (S5) with frame compare with plate (S11) without frame 104% , 134% and 410% increasing in initial cracking load and ultimate load but decrease in ductility index and energy absorbtion by 64% and 11% as shown in Figure 38.

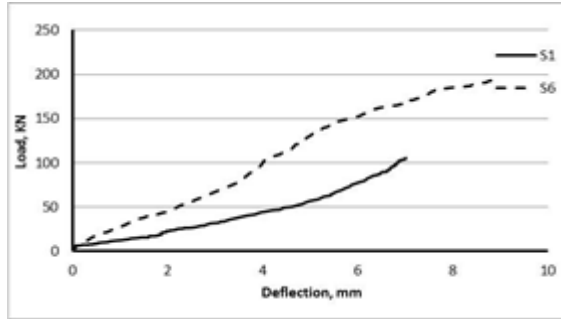


Figure 34: effect of using web for the plates with two layer of welded steel mesh and traditional reinforcement .

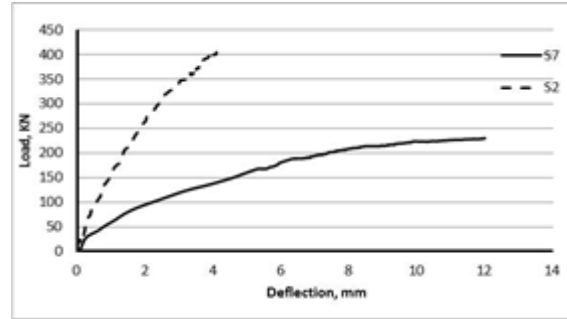


Figure 35: effect of using web on the load-deflection for the plates with four layer of welded steel mesh only.

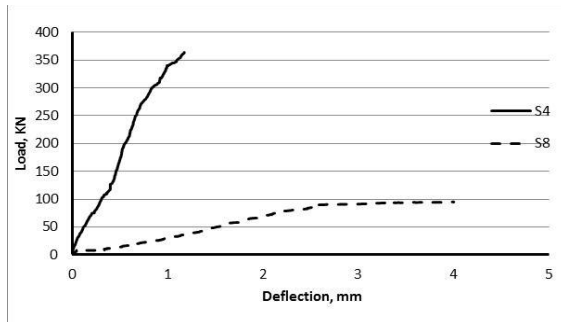


Figure 36: effect of using web on the load-deflection for the plates without welded steel mesh.

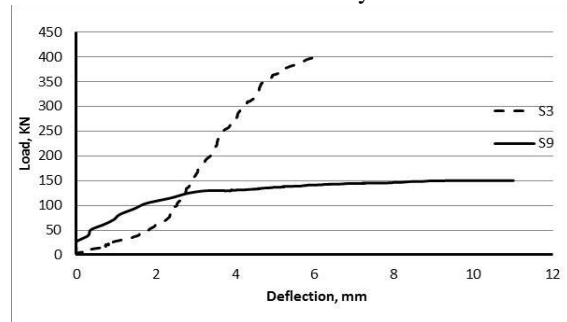


Figure 37: effect of using web on the load-deflection for the plates with steel and three layer of welded steel mesh

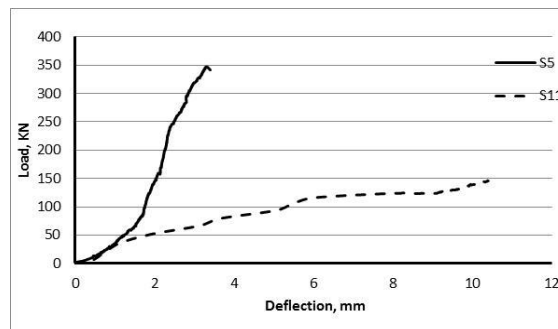


Figure 38: effect of using web on the load-deflection for the plates with three layer of welded steel mesh only.

4.4 Effect of direction of loading

The effect of direction of web is shown in Figure 39. It is noticed that the initial cracking, ultimate load and energy absorptions increased by 55% , 91% and 989% for the plate (S3) which was loaded perpendicular to the web compared with plate (S12) which was loaded parralar to web .

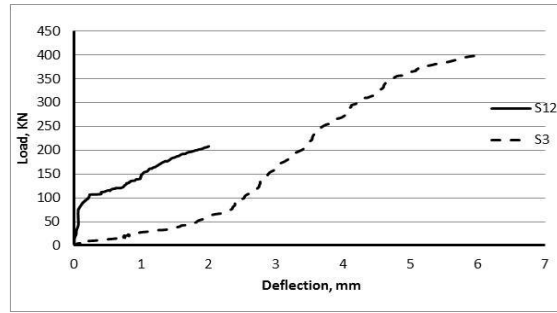
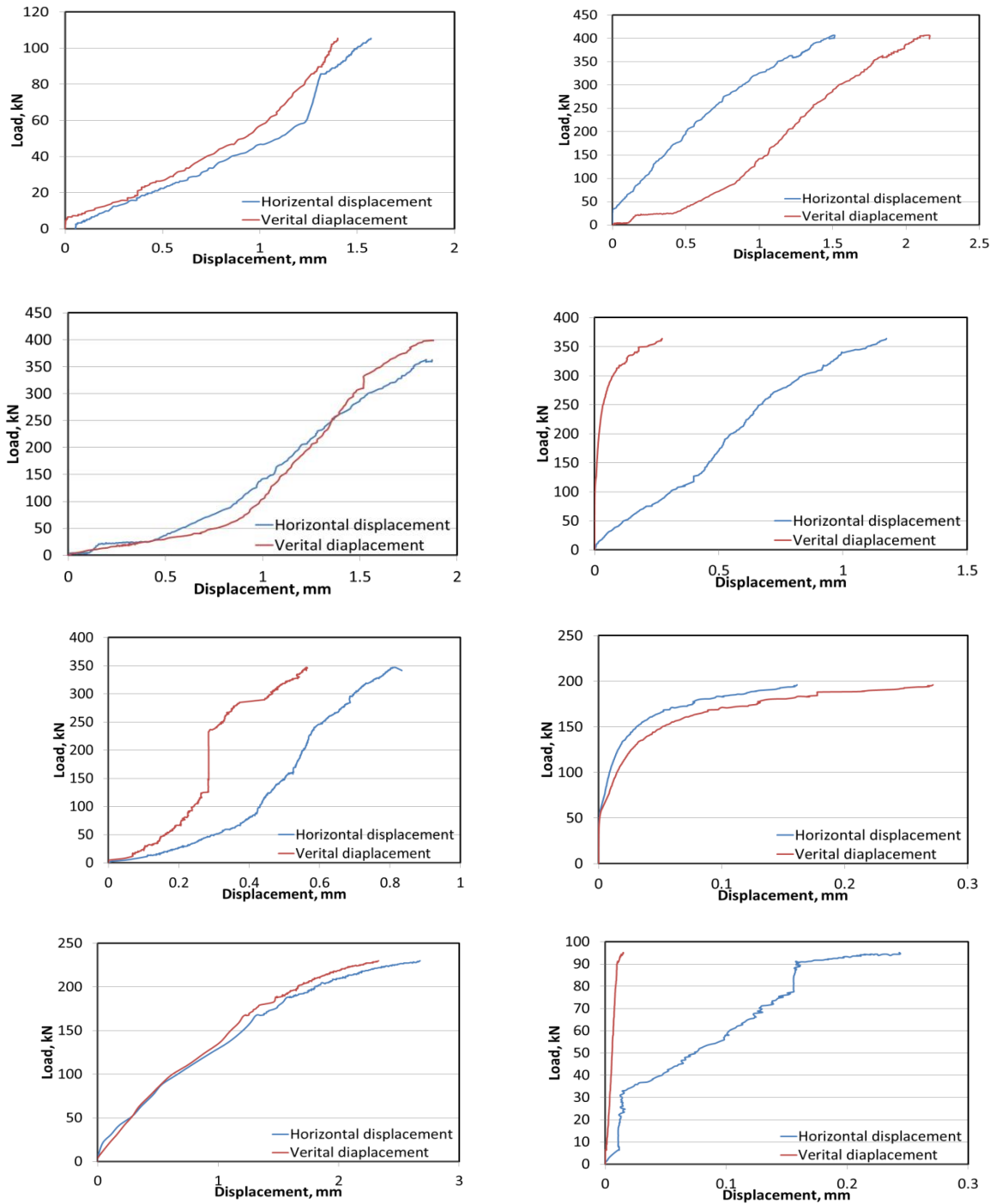


Figure 39: Effect of direction of loading with inner frame



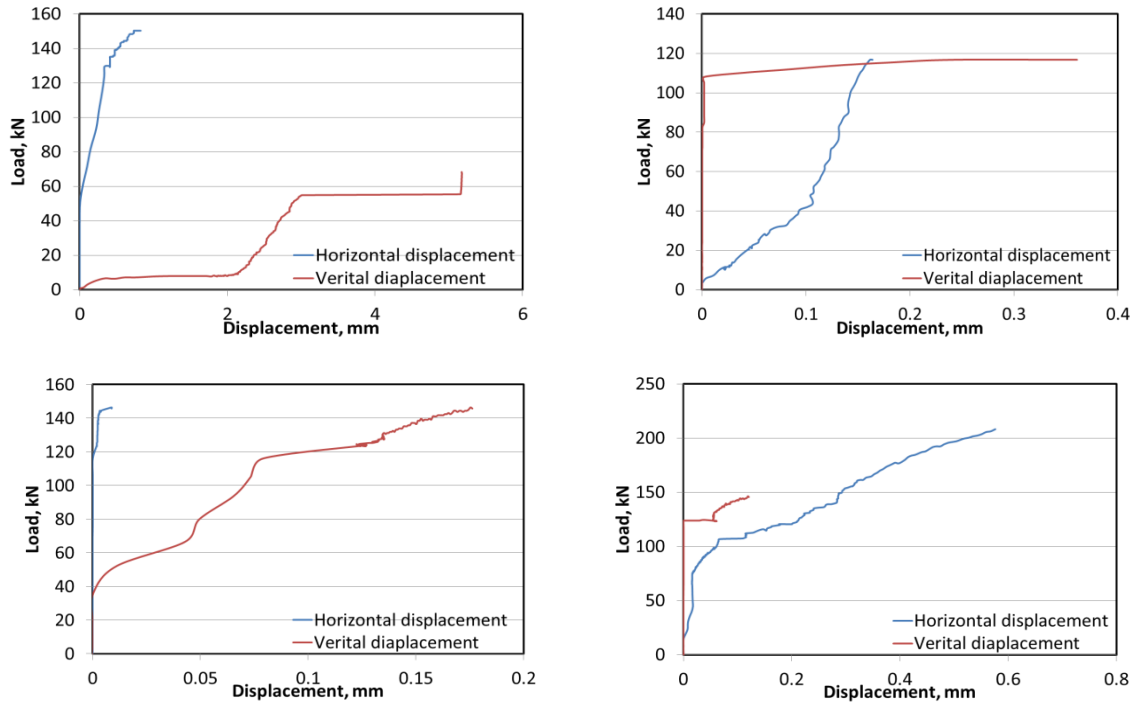


Figure 40: Displacement for the tested plates.

4.5 Ductility index and Energy absorption

The test results are listed in **Table 9**. The table shows the obtained experimental results for each specimen as well as the ductility ratio, and energy absorption properties. Ductility ratio is defined here as the ratio between the mid-span deflection at ultimate load to that at the first crack load (Δ_u/Δ_y), while the energy absorption is defined as the area under the load-deflection curve. Computer program (BASIC language) was used to calculate the area under curve by integrated the equation of the load-deflection curve for each beam specimens as follow: ultimate load Energy absorbed = $\int_0^{\Delta_u} f(\Delta) d\Delta$; Where $f(\Delta)$ is the equation of load-deflection curve, and Δ_u is the mid-span deflection at failure load. The value of energy absorption and ductility index for all plates is presented in Table 9. It was observed the ductility behavior of the plates reinforced with wire meshes had ductility ratio more than with steel reinforcement because of volume fruction . The ductility ratio for the test specimens ranged from 1.9 to 35.35 .The energy absorption of tested plates reinforced with steel wire meshes was higher than that with steel reinforcement volume fruction. Ductility index and energy absorption increased as the number of layers of steel wire meshes were increasing. This illustrates the effect of the stiffness of the plates

5. Crack pattern

Cracking patterns for all the tested plates were illustrated in figure 41. All tested plates were un-cracked beam for the initial stages of loading . When the applied load reached to the rupture strength of the concrete on specimen, the concrete started to crack up to the failure pattern in the all tested plates.



Figure 41 : Cracking pattern of tested plates.

6. Finite Element Model

A finite element package (ANSYS version 15), was used to simulate the behavior of thin ferrocement plates. Two types of elements were used; solid 65 and link 8. The SOLID65 3-D Reinforced Concrete Solid. Link 8 which were defined by two nodes, the cross-sectional area, an initial strain, and the material properties. The element x-axis is oriented along the length of the element from node I toward node J. The steel wire meshes was defined by the volume fraction, initial strain and the material properties. Figure 42 to Figure 47 show the configurations of tested plates and theoretical results for the ANSYS program. A comparison between experimental and numerical results is shown in table 10.

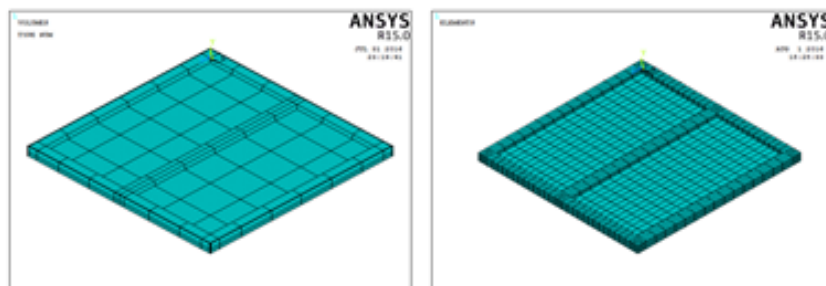


Figure 42 : The Configuration of the tested plates.

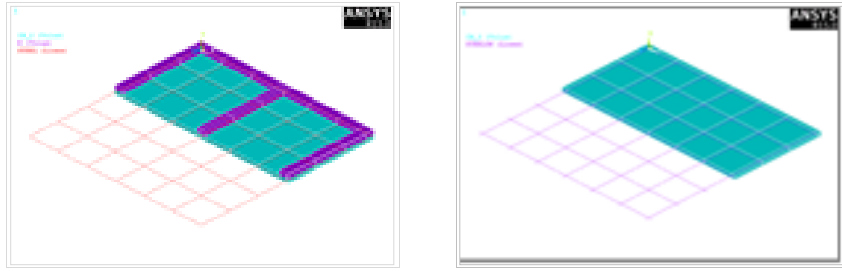


Figure 43: Reinforcement of tested plates

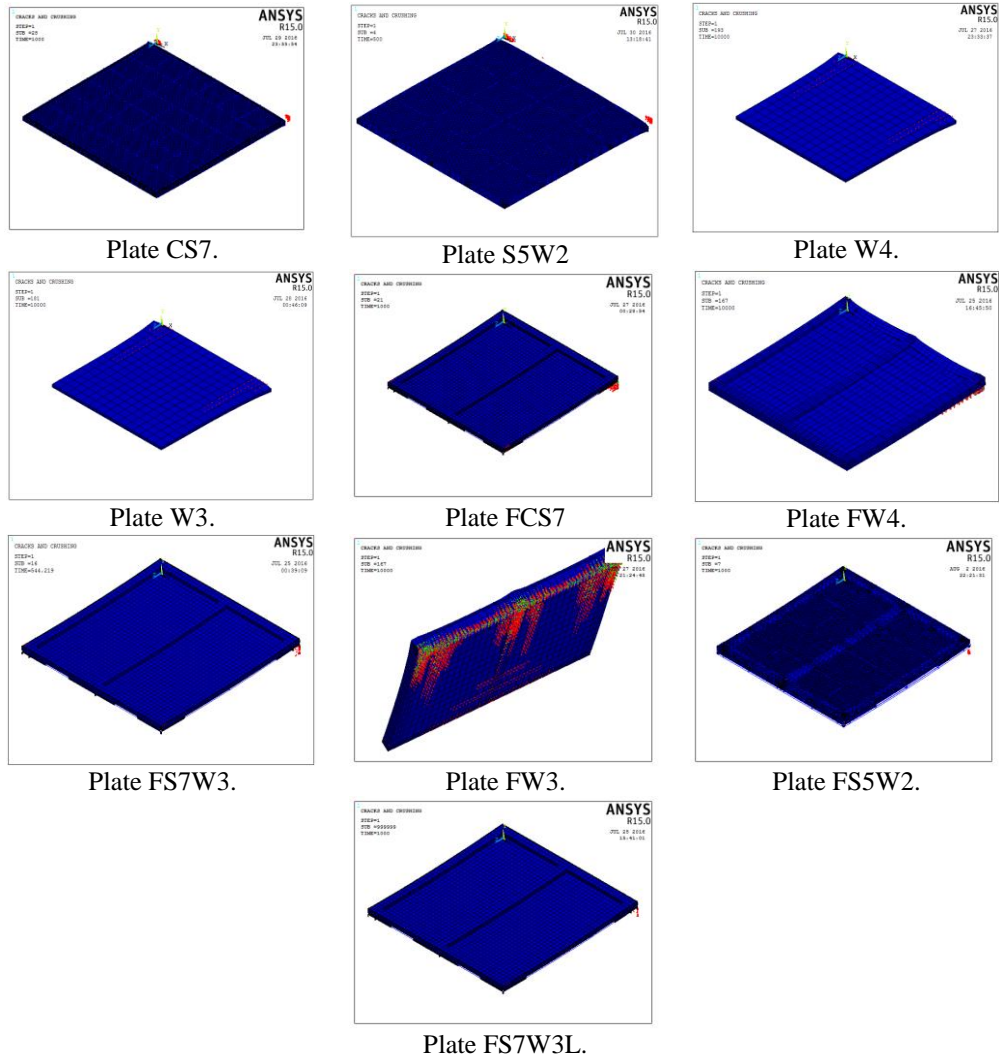


Figure 44 : The cracks and crushing pattern different plates

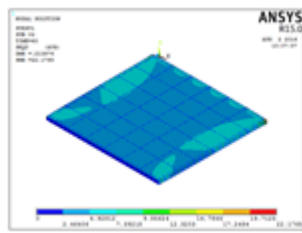


Plate CS7.

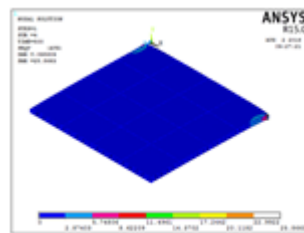


Plate S5W2.

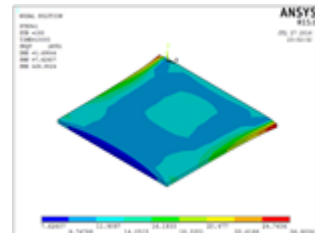


Plate W4.

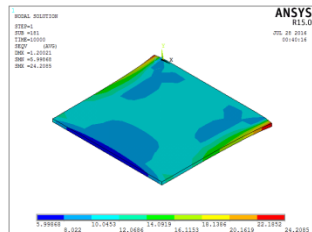


Plate W3.

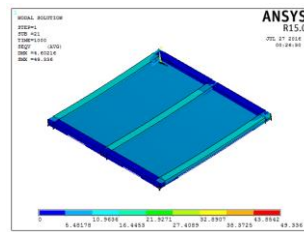


Plate FCS7.

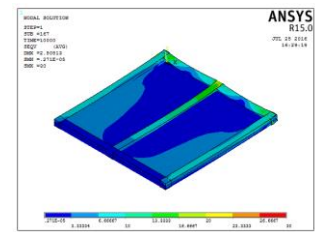


Plate FW4.

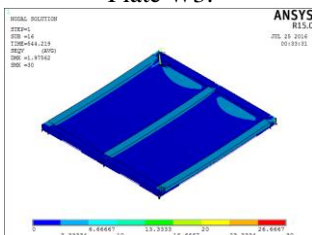


Plate FS7W3.

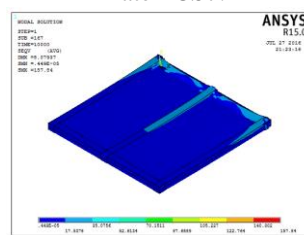


Plate FW3.

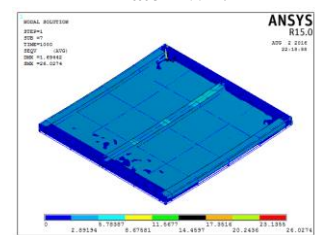


Plate FS5W2.

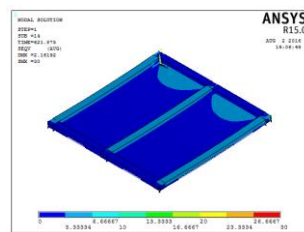


Plate FS7W3L

Figure 45 : Stress distribution (nodal solution) for different plates.

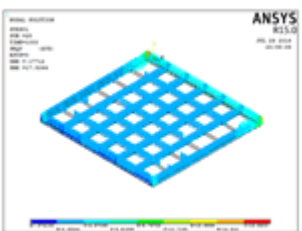


Plate CS7.

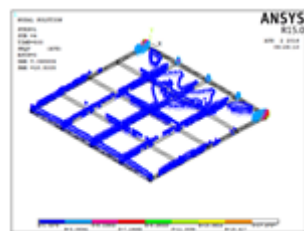


Plate S5W2.

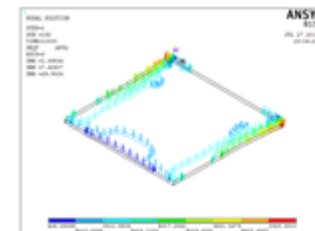


Plate W4.

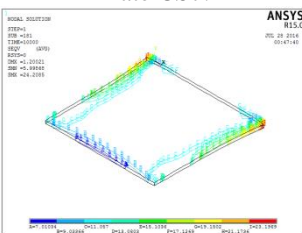


Plate W3.

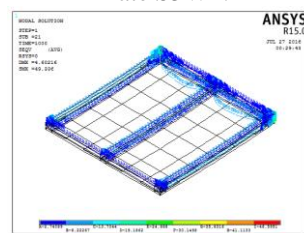


Plate FCS7.

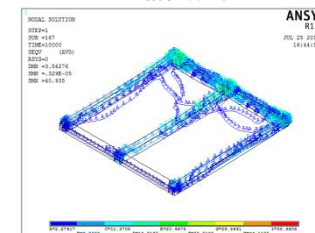


Plate FW4.

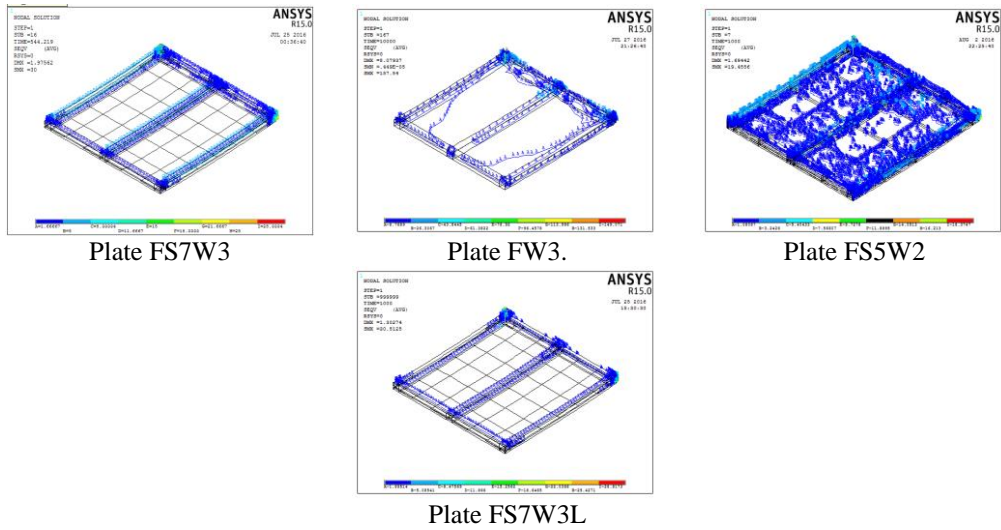


Figure 46 : Stress distribution (nodal solution2) for different plates

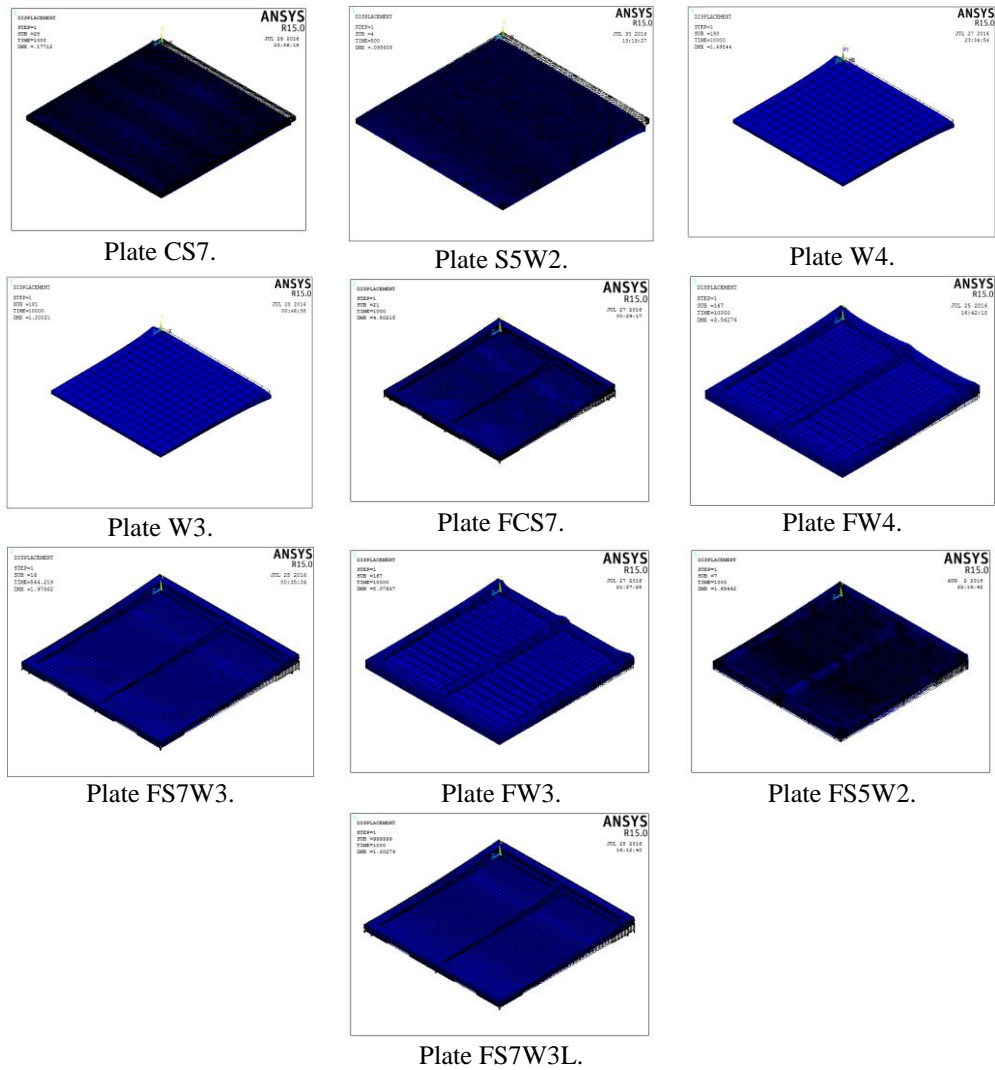


Figure 47 : Displacement for different plates

Table 10: Comparison between the ultimate load of the experimental and the theoretical results.

Code	$P_{exp.}$ kN	$P_{theo.}$ kN	$P_{exp.} / P_{theo.}$
S5W2	105	115	109%
FW4	406	420	103%
FS7W3	398	415	104%
FCS7	363	375	103%
FW3	346	361	104%
FS5W2	193	207	107%
W4	230	238	103%
CS7	95	109	114%
S7W3	150	159	106%
S7W2	116	108	92%
W3	146	152	104%
FS7W3L	208	214	103%

Conclusions:

1. Based on the results and observations of the experimental work illustrated in this paper, the following conclusions could be drawn:
2. Because of the lighter and easier handling and easier bedding of welded steel wire mesh compared with steel reinforcement; welded wire mesh offers numerous advantages especially for structures with complex shapes.
3. Grate improving was noticed with behaviour when using welded steel wire mesh as reinforcement.
4. Due to the presence of the web frame for the plate increased initial cracks, ultimate load and energy absorption.
5. Increasing the volume fraction of the reinforcement increased the initial cracks, ultimate loads, energy absorption and ductility index.
6. Cracks with greater number and narrower widths were observed for those plates reinforced with welded steel wire meshes compared with the plates reinforced with steel reinforcement.
7. 145 %, 84% , 6 % and 76% increasing in initial cracking load, ultimate load, ductility index and energy absorption, respectively for plate with frame compared with plate (S1) without frame.
8. A decreasing in the initial cracking and increasing ultimate load by 21% and 17 % for the plates reinforced with conventional reinforcement compared with reinforced with four layers belong to framed plates
9. the energy absorbed was increased by 327% for the plates reinforced with four layers of steel wire meshes compared with the plates reinforced with conventional reinforcement belong to framed plates
10. The energy absorption and ductility index increased by 10% and 208% for the plate reinforced with four layers compared with the plates reinforced with three layers belong to framed plates
11. the initial cracking, ultimate load and energy absorptions increased by 55% , 91% and 989% for the plate which was loaded perpendicular to the web compared with plate which was loaded parallel to web .
12. Good agreement between the theoretical results and the experimental results

References

- [1] ACI Committee 549. State-of-the-Art report on ferrocement". ACI549-R97, in manual of concrete practice. ACI, Detroit, 1997, 26pp..(reapproved 2009)
- [2] A. Koukousel and E. Mistakid, "Buckling Behavior of Composite Ferrocement Plates" Conference: 8th Hellenic National Conference of Steel Structures, October 2014
- [3] P.B. Sakthivel and A. Jagannathan , "Ferrocement Construction Technology and its Applications – A Review" <http://dl.lib.mrt.ac.lk/handle/123/9492>
- [4] M. N. Savale and P. M. Alandkar "Shear behaviour of ferrocement plates"International Journal of Innovative Research in Science, Engineering and Technology Vol. 2, Issue 2, February 2013
- [5] A.W. Hago, K.S. Al-Jabri, A.S. Alnuaimi, H. Al-Moqbali and M. A. Al-Kubaisy (2005). "Ultimate and Service Behavior of Ferrocement Roof Plate Panels." Constr. Build. Mater. 19:31–37.
- [6] Ibrahim HM (2011) "Experimental Investigation of Ultimate Capacity of Wired Mesh-Reinforced Cementitious Plates." Constr. Build. Mater. 25:251–259.
- [7] H. M. Ibrahim (2011). "Shear Capacity of Ferrocement Plates in Flexure." Eng. Struct. 33:1680–1686.
- [8] H. H. Nassif, H. Najm (2004) "Experimental and Analytical Investigation of Ferrocement–Concrete Composite Beams." Cem. Concrete Compos. 26:787-796.
- [9] S. Bhalsing, S. Shoaib and P. Autade "Tensile Strength of Ferrocement with respect to Specific Surface" international journal of innovative research in science, engineering and technology volume 3, Special Issue 4, April 2014
- [10] J.A. Desai (2011) "Corrosion and Ferrocement", Proceedings of the National Conference on Ferrocement, FS 2011, 13-14 May 2011, Pune, India,, pp.45-52.
- [11] B. N. Divekar (2011c) —Research Needs in Ferrocement Technology, Proceedings of the National Conference on Ferrocement, FS 2011, 13-14 May 2011, Pune, India, 227-228.
- [12] B. Kondraivendhan and B. Pradhan (2009) "Effect of ferrocement confinement on behavior of concrete", Constr Build Mater, 23(3):1218–22.
- [13] Egyptian Standards Specification, E.S.S, 4756-11, 2009, (physical and mechanical properties examination of cement, part 1), Cairo, 2009.
- [14] ASTM C494/C 494M, Standard Specification for Chemical Admixtures for Concrete, Annual Book of ASTM Standards 2001, 04, 02, p.9.
- [15] ASTM C1116/C1116M – 10a. Standard Specification for Fiber- Reinforced Concrete, p. 7.